



저작자표시 2.0 대한민국

이용자는 아래의 조건을 따르는 경우에 한하여 자유롭게

- 이 저작물을 복제, 배포, 전송, 전시, 공연 및 방송할 수 있습니다.
- 이차적 저작물을 작성할 수 있습니다.
- 이 저작물을 영리 목적으로 이용할 수 있습니다.

다음과 같은 조건을 따라야 합니다:



저작자표시. 귀하는 원저작자를 표시하여야 합니다.

- 귀하는, 이 저작물의 재이용이나 배포의 경우, 이 저작물에 적용된 이용허락조건을 명확하게 나타내어야 합니다.
- 저작권자로부터 별도의 허가를 받으면 이러한 조건들은 적용되지 않습니다.

저작권법에 따른 이용자의 권리는 위의 내용에 의하여 영향을 받지 않습니다.

이것은 [이용허락규약\(Legal Code\)](#)을 이해하기 쉽게 요약한 것입니다.

[Disclaimer](#) 

Edge-iodine/sulfonic acid functionalized graphene
nanoplatelets as an efficient electrocatalyst for
oxygen reduction reaction

Jong Yeol Baek

Department of Energy Engineering

Graduate School of UNIST

2015

Edge-iodine/sulfonic acid functionalized graphene
nanoplatelets as an efficient electrocatalyst for
oxygen reduction reaction

Jong Yeol Baek

Department of Energy Engineering

Graduate School of UNIST

Edge-iodine/sulfonic acid functionalized graphene
nanoplatelets as an efficient electrocatalyst for
oxygen reduction reaction

A thesis/dissertation
submitted to the Graduate School of UNIST
in partial fulfillment of the
requirements for the degree of
Master of Science

Jong Yeol Baek

1. 8. 2015

Approved by



Major Advisor

Jong-Beom Baek

Edge-iodine/sulfonic acid functionalized graphene
nanoplatelets as an efficient electrocatalyst for
oxygen reduction reaction

Jong Yeol Baek

This certifies that the thesis of Jong Yeol Baek is approved.

1. 8. 2015

signature



Supervisor: Jong-Beom Baek

signature



Hyun-Kon Song

signature



Soojin Park

Abstract

Development of electrocatalysts, along with cheap and available materials to facilitate oxygen reduction reaction (ORR) in fuel cells to replace Pt-based catalyst is an important issue in the development of fuel cells and other electro-chemical energy devices. The graphene provides good substitutes for electrode catalyst and some research have done to apply graphene nano-material into an cathodic catalyst as an ORR performance owing to its large surface area, the excellent conductivity, freely selectable functional groups such as atoms, molecules involved. It also can be noted that well-defined theoretical design of graphene-based nano-material with specific structure can perform important electro-chemical property in fuel cells ORR. Many studies have made for various hetero-atom based graphene nano-material or graphene-based nano-composites to reach goals which is its extraordinary characteristics for applications (ORR) in the fuel cells. It is reported that the synthesis of edge-iodine/sulfonic acid functionalized graphene nanoplatelets (ISGnP) *via* two-step sequential ball-milling graphite and their use as electrocatalyst for oxygen reduction reaction (ORR) in fuel cells. Graphite was ball-milled in presence of iodine to produce edge-iodine functionalized GnP (IGnP) in the first step and subsequently IGnP was ball-milled with sulfur trioxide to yield ISGnP. The resultant ISGnP was highly dispersible in various polar solvents, allowing the fabrication of electrodes for ORR using solution processing. The ORR performance of ISGnP in an alkaline medium was superior to commercial Pt/C in terms of electrocatalytic activity and cycle stability.

Contents

I.	Introduction-----	
II.	Experiment-----	
2.1	Materials-----	
2.2	Instrumentations-----	
2.3	Procedure for the preparation of ISGnP by stepwise ball-milling graphite in the presence of iodine and sulfur trioxide-----	
2.4	Electro-chemical study-----	
III.	Results and discussion-----	
3.1	Structural information-----	
3.1.1	Functionalization of graphite via ball-mill and Morphology of pristine graphite and IS-graphite-----	
3.1.2	FT-IR study-----	
3.1.3	Elemental analysis (EA), X-ray photoelectron spectroscopy (XPS) and Energy dispersive X-ray (EDX) study-----	
3.1.4	Thermal properties (Thermogravimetric analysis (TGA))-----	
3.1.5	Raman spectroscopy study-----	
3.1.6	X-ray diffraction (XRD) study-----	
3.1.7	Dispersion stability test, Zeta-potential Study, Contact angle study-----	
3.2	Application (Oxygen reduction reaction)-----	
3.2.1	Cyclic voltammetry (CV)-----	
3.2.2	Rotating disk electrode (RDE)-----	

IV. Conclusions

References

List of figures

Figure 1. (a) Schematic representation of stepwise ball-milling graphite in the presence of (1) iodine and (2) sulfur trioxide to produce ISGnPs. SEM images: (b) pristine graphite; (c) ISGnP. Scale bars are 1 μm .

Figure 2. FT-IR spectra.

Figure 3. XPS survey spectrum

Figure 4. High-resolution XPS survey spectra of the ISGnP: (a) C 1s; (b) O 1s; (c) S 2p; (d) I

Figure 5. TGA results obtained at the rate of 10 $^{\circ}\text{C}/\text{min}$: (a) in air; (b) in nitrogen.

Figure 6. Raman spectrum.

Figure 7. XRD results

Figure 8. Photographs of ISGnP dispersed solutions in various solvents after one week standing on bench top in the normal laboratory condition: (a) (1) H_2O ; (2) 1M aq. NH_4OH ; (3) 1M aq. HCl ; (4) MeOH ; (5) EtOH ; (6) ethyl acetate; (7) acetone; (8) DMAc ; (9) DMF ; (10) NMP ; (11) toluene; (12) CH_2Cl_2 ; (13) hexane; (14) diethyl ether; (15) THF . Contact angles: (b) the surface of ISGnP coated on Si wafer; (c) the surface of Si wafer. The contact angle is an average value of ten measurements.

Figure 9. Cyclic voltammograms (CV) of samples on glassy carbon (GC) electrodes in 0.1 M aq. KOH solution; with scan rate of 10 mV/s : (a) Nitrogen-saturated; (b) Oxygen-saturated.

Figure 10. Comparison of cyclic voltammograms (CV) of samples on glassy carbon (GC) electrodes in 0.1 M aq. KOH solution with scan rate of 100 mV/s: (a) ISGnP in nitrogen-saturated condition; (b) ISGnP in oxygen-saturated condition; (c) Pt/C in nitrogen-saturated condition; (b) Pt/C in oxygen-saturated condition.

Figure 11. Koutecky-Levich plots derived from RDE measurements at different electrode potentials: (a) Pristine graphite; (b) ISGnP; (c) Pt/C; (d) Comparison of the Koutecky-Levich plots at -0.6 V electrode potential. ISGnP and Pt/C are a four-electron transfer process, while the pristine graphite is close to a classical two-electron process.

Figure 12. RDE voltammograms in oxygen-saturated 0.1 M aq. KOH solution with a scan rate of 10 mV/s at different rotating rates of 400, 600, 900, 1200, 1600, 2000 and 2500 rpm: (a) the pristine graphite; (b) ISGnP; (c) Pt/C; (d) comparison of RDE voltammograms of sample electrodes at a rotation rate of 1600 rpm.

List of tables

Table 1. TGA residue amount (%) in N₂ flow at 800 °C, 1000 °C respectively and EA, EDX, XPS of the pristine graphite and ISGnP

Table 2. Zeta-potential of samples at different concentrations in NMP solution

Table 3. The relationship between Zeta-potential and colloidal stability*

Table 4. The specific capacitance (F/g) obtained from average value of 100 cycles

Table 5. BET surface areas of samples

Table 6. The cycle retention after 10000 cycles in oxygen- and nitrogen-saturated 0.1M aq. KOH electrolyte at the scan rate of 100 mV/s

Table 7. The average number of electrons (n) transferred for oxygen reduction reaction at different potential for sample electrodes in oxygen-saturated 0.1M aq. KOH electrolyte

List of Schemes

Scheme 1. Various graphene-based nano-material as electro-chemical catalyst for ORR

Scheme 2. Fuel cells work by electro-chemically decomposing fuel instead of burning it, converting energy directly into electricity.

Scheme 3. A Scheme of mechanochemical reaction (ball-mill synthesis) between in-situ generated highly active carbon atoms and introduced reactant gases into the ball mill reactor. The cracking, cleavage of graphite by ball-mill under desired, interesting gases and subsequent exposure to air containing moisture results in the formation of Edge-Functionalized graphene nanoplatelets (EFGnP).

Nomenclature

EFGnP: Edge-functionalized graphene nanoplatelets

ISGnP: Iodine/Sulfonic acid functionalized graphene nanoplatelets

HGnP: Hydrogen functionalized graphene nanoplatelets

ORR: Oxygen reduction reaction

Pt: Platinum

Pt/C: Platinum(Pt) on activated carbon

GC: Glassy carbon

D.I. water: Distilled water (Deionized water)

CVD: Chemical vapor deposition

GO: graphite oxide

rGO: Reduced graphite oxide

CNT: Carbon nanotube

EA: Elemental analysis

XPS: X-ray photoelectron spectroscopy

EDX: Energy dispersive X-ray

SEM: Scanning electron microscope

FT-IR: Fourier-transform Infrared

TGA: Thermogravimetric analysis

XRD: X-ray diffraction

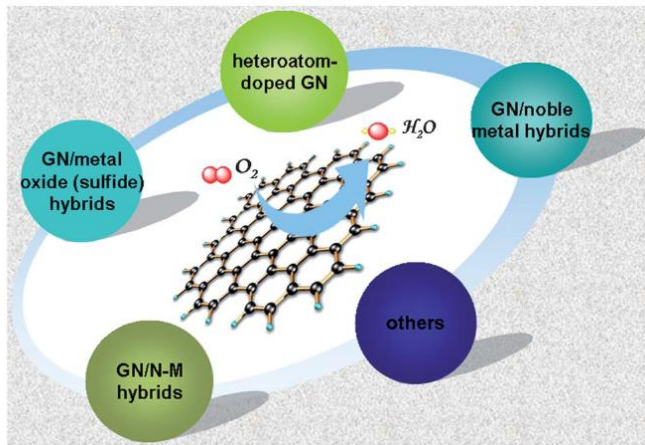
CV: Cyclic voltammetry

RDE: Rotating disk electrode

I. Introduction

Energy demand is expected to increase considerably as a result of population growth and economic development. Therefore, the great effort for alternative sustainable energy technology has been going on. Various ongoing electro-chemical energy generating system (fuel cells, supercapacitors and Li ion batteries) are substitutes. For fuel cells, the cathodic catalyst which is related with the oxygen reduction reaction (ORR) performs important things for determining the characteristics of electro-chemical based energy devices such as fuel cells.

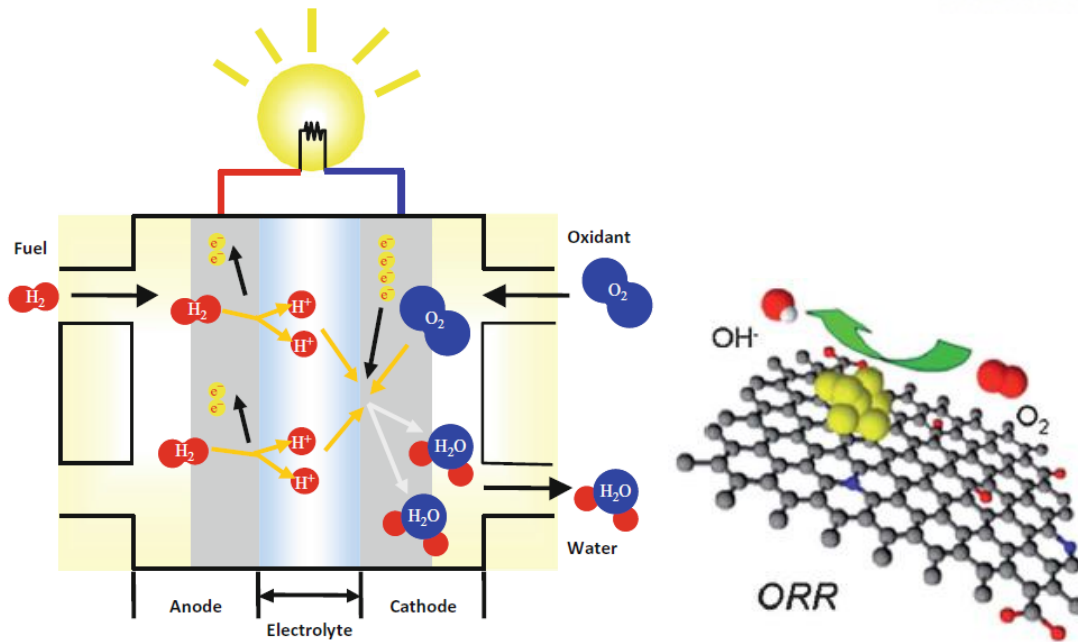
Platinum is widely utilized as the fuel cell catalysts in ORR. Yet, some important issues should be issued until Pt catalysts can be commercialized in a practical utilization. The absolute fact is the slow ORR kinetics should require high amount Pt loading onto the cathode to get a large amount of the energy generating system within short time. Furthermore, the Platinum active material suffers from its poor durability because of drift and carbon monoxide, methanol deactivation (oxidation). It drastically decreases the cathodic potential (onset potential) and conversion efficiency in fuel cells. More, the high cost of Pt catalysts limited reserves in nature, has shown for one of the major obstacle to global energy device market in commercialization. Under the worldwide situations, the fuel cells catalyst development for enhancing ORR performance should be very urgent, desired. Due to the expensive Pt cost, time-drift poor performance as previously mentioned, the fuel cells catalyst related with organic carbon based materials through doping hetero-atom into graphitic structure¹ or other co-doped metal/organic carbon material have been actively studied up to now.



Scheme 1. A variety of graphene-based nano-material for electro-chemical catalyst in ORR

Based on the specific, unique characteristics of graphene, many research efforts have been conducted to synthesize graphene-based nano-material for enhanced performance in fuel cells ORR. By the way,

the theoretical, experimental researches have been done until now. The both studies have shown heteroatom-based graphene nano-material (a nitrogen, a sulfur, halogen atoms) can modulate their electronic properties such as band gap, conductivity and chemical reactivity such as reactivity, solubility to accelerate electro-catalytic, chemical activities, as well as rise to new functions, which could be regarded to be promising cheap, excellent performing electrocatalysts for ORR in fuel cell. There are numerous approaches to prepare the heteroatom-doped carbon nano-materials. A representative research example is Nitrogen doped graphene (N-graphene). It exhibits excellent electro-catalytic activity, electro-chemical tolerance under Methanol, CO against oxidation on cathode in a comparison with existing Pt based catalyst in ORR fuel cells, exhibit absolute promising in future energy to replace Pt based precious catalyst in ORR fuel cells. It also can influence other electro-chemical device fields. However, metal based catalyst still suffers from electrolyte dissolution, poisoning, time-drift aggregation during their operations. They could affect to degraded, poor catalysts. Most cases, the poor conductivity of these metal oxide based electro-catalysts constitutes one of the major bottlenecks in application in electrical energy system because electron flows into the electrodes are significantly perturbed in the catalytic process. When considering its excellent thermal, electrical conductivity and broad surface area, graphene-based material have appeared now for the new catalyst alternative. When considering important component in graphene nano-composite functionality. The application of graphene can improve the catalytic-active graphene surface area efficiently, enhance its conductivity. It also can improve its catalytic performance via electronic modulation, tolerance under Methanol, CO. The GO which is the precursor of graphene, could show good solubility or dispersion in various organic solvents and provide additional applications to construct graphene related hybrid type nano-composite, its latent application as excellent electro-catalyst for in ORR fuel cells. As mentioning again, graphene would not only show for the high performance organic electrocatalyst but also can be adopted as a catalyst substitute for novel metal such as Pt.

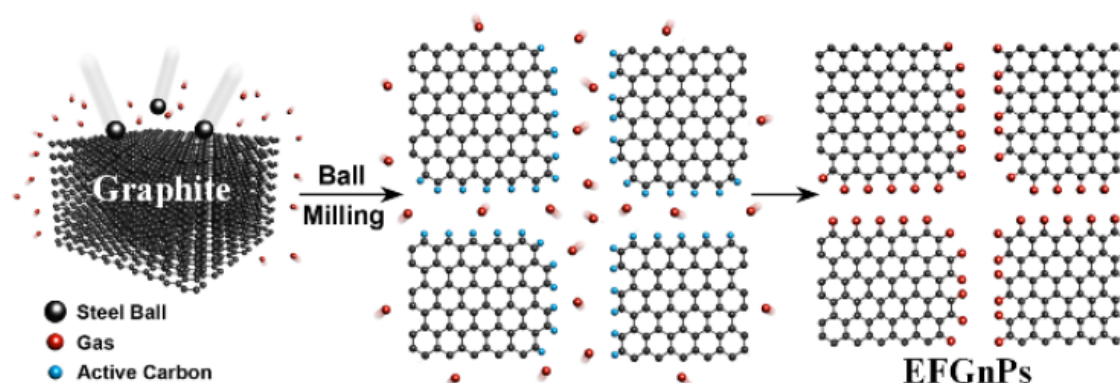


Scheme 1. Fuel cells work by electro-chemically decomposing fuel instead of burning it, converting energy directly into electricity.

It is necessary to open up theoretical designs in the graphene nano-material, along with well-defined structure. The point would perform some important roles for the electro-chemical performance in ORR fuel cells. Many studies have made to construct various hetero-atom doped graphene nano-material or graphene-based nano-composite, fully aiming at using its excellent properties for ORR applications. Under these important views, in harmony with theoretical structural design, application studies and recent ongoing research advancements as the graphene-based electrocatalyst development for ORR performance in electro-chemical energy generation device (fuel cells & secondary batteries) have an attention up to now. For example; heteroatom-doped graphene nano-materials, nonprecious graphene-based hybrid type (graphene/metal-oxide, graphene/Nano-material composite, graphene/calcoenic atoms etc.) and Graphene nanoplatelets/noble metal (Pt) nano-composite.

Hetero-atom doped graphene would be synthesized in a variety of methods:

1. Chemical vapor deposition (CVD): a carbon backbone, together with other species are vaporized, deposited onto a support substrate.
2. Arc discharge: graphite electrode vaporized in the presence of an atom such as nitrogen and other precursor results in hetero-atom doped graphene.
3. Solvothermal reaction: it mixes desired precursors, solvent in a sealed, high pressure autoclave. After then, it heats the mixture to specific temperature for specific time.
4. Ball-milling: A recent technique involving ball milling of graphite in the presence of a variety of gaseous elements to produce edge functionalized graphene nanoplatelets
5. Thermal treatment: In a typical thermal treatment, nitrogen atom can be introduced by exposing the carbon material to a nitrogen-rich atmosphere under high temperature.
6. Reduction of graphene oxide(GO): A $N_2H_4-NH_3$ mixture can be used reduce and nitrogen doped GO at usually the temperature lower than $160^\circ C$



Scheme 3. A Scheme of mechanochemical reaction (ball-mill synthesis) between in-situ generated highly active carbon atoms and introduced reactant gases into the ball mill reactor. The cracking, cleavage of graphite by ball-mill under desired, interesting gases and subsequent exposure to air containing moisture results in the formation of Edge-Functionalized graphene nanoplatelets (EFGnP).

Representatively, several approaches including chemical vapor deposition (CVD),¹ the chemical derivatization of graphite oxide (GO)² have been investigated for the introduction of heteroatoms such as boron,³ pnictogens,⁴ chalcogens⁵ and halogens⁶ into graphitic frameworks. Although CVD method can produce high quality doped graphene nanoplatelets (GnPs),³ it requires meticulous technical elaborations and thus it is not cost-effective for a scalable production to be uses in practice. The solution exfoliation of graphite into GO allows the mass production of GnPs. However, the method involves strong hazardous oxidizing reagents (e.g., HNO_3 , $KMnO_4$, and/or H_2SO_4) and a

tedious multi-step process.⁷ After the exfoliation of graphite into GO, a reduction of GO into reduced graphene oxide (rGO) requires even more hazardous reducing reagents (e.g., hydrazine, NaBH₄).^{4,8,9} These treatments, which use strongly destructive reagents lead to severe physical and chemical damages to the graphitic framework, diminish unique properties such as electrical characteristics and structural integrity arising from high crystallinity of graphitic structure.¹⁰ Recently, it has been developed an alternative method to overcome the limitations of CVD and GO approaches. The newly-developed mechanochemical ball-milling can introduce various functional groups at the cracked edges of GnPs.¹¹ The mechanism involves that mechanochemical cracking of graphitic C-C bonds generates reactive carbon species, which induce edge-selective functionalization at the cracked edges and subsequent delamination of graphitic layers into a few layer GnPs. As a result, the mechanochemical process is a simple, but low-cost, eco-friendly, scalable approach to produce various GnPs with desired functionality and minimal distortion of basal plane.^{13,12,13,14} On the basis of an optimized condition for mechanochemical process, It could be hybridized two systems for the best electrocatalytic activity for oxygen-reduction reaction (ORR) in fuel-cells. Iodine group in edge-iodine/sulfonic acid functionalized GnPs (ISGnP) thermodynamically contributed to the charge polarization for enhanced ORR performance¹⁵ and sulfonic acid group in ISGnP kinetically attributed to the efficient oxygen diffusion for improved ORR performance.¹⁴ As a result, the ISGnP was expected to exhibit synergistically enhanced ORR performance. Thus, ISGnP was prepared by two-step sequential ball-milling graphite in the presence of iodine in the first step and sulfur trioxide in the following step. The resultant ISGnP is dispersible well in many polar solvents, leading to feasible solution process for many practical applications. In this work, metal-free cathodes were fabricated for fuel cell application. The ISGnP displayed high electrocatalytic activity in an alkaline electrolyte (0.1M KOH), which is superb to Pt-based electrocatalyst in terms of current density and cycle stability for use in practice

II. Experiment

2.1 Materials

All reagents and were purchased from Aldrich Chemical Inc. or Alfa Aesar, USA. and used as received, unless otherwise specified. The pristine graphite (natural graphite, 100 mesh, < 150 μm , 99.9995% metals basis, lot # 14735) was obtained from Alfa-aesar. and Iodine ($\geq 99.8\%$), sulfur trioxide ($\geq 99.0\%$) were also obtained from Aldrich Chemical Inc.

2.2 Instrumentations

Fourier transform infrared (FT-IR) spectra were recorded on Perkin-Elmer Spectrum 100 using KBr pellets. TGA were conducted on a TA Q200 (TA Instrument) under air and nitrogen atmosphere with a ramping rate of 10 $^{\circ}\text{C}/\text{min}$. The surface area was measured by nitrogen adsorption–desorption isotherms using the Brunauer–Emmett–Teller (BET) method on Micromeritics ASAP 2504N. The field emission scanning electron microscopy (FE-SEM) was performed on FEI Nanonova 230. X-ray photoelectron spectra (XPS) were recorded on a Thermo Fisher K-alpha XPS spectrometer. Elemental analysis (EA) was conducted with Thermo Scientific Flash 2000. X-ray diffraction (XRD) patterns were recorded with a Rigaku D/MAZX 2500 V/PC with Cu–K α radiation (35 kV, 20 mA, $\lambda = 1.5418 \text{ \AA}$). Raman spectra were taken with a He–Ne laser (532 nm) as the excitation source by using confocal Raman microscopy (Alpha 300S, WITec, Germany). Contact angle measurements were conducted on a Krüss DSA 100 contact angle analyzer. Sample solutions were coated on a silicon (Si) wafer.

2.3 Procedure for the preparation of ISGnP by stepwise ball-milling graphite in the presence of iodine and sulfur trioxide.

In a typical experiment, the ball-milling graphite was carried out in a planetary ball-mill machine (Pulverisette 6, Fritsch) in the presence of the iodine and sulfur trioxide at 500 rpm for 24 hours for each step. For the first step, the pristine graphite (5.0 g, Alfa Aesar, natural graphite, 100 mesh, < 150 μm , 99.9995% metals basis, lot # 14735) and iodine (10.0g, Aldrich Chemical Inc., $\geq 99.8\%$) were placed into a stainless steel capsule containing stainless steel balls (500 g, diameter: 5 mm). After five cycles of argon charge/discharge through gas inlet, the capsule was fixed in the ball-mill machine and agitated with 500 rpm for 24 h. The intermediate edge-iodine functionalized graphene nanoplatelets (IGnP) were completely worked-up by Soxhlet extracted with 1 M aq. HCl solution to completely acidify the residual active species and to remove metallic impurities (*e.g.*, iron oxide), if any. Further Soxhlet extraction with methanol was conducted to get rid of residual iodine. The resultant IGnP was freeze-dried at $-120 \text{ }^{\circ}\text{C}$ under a reduced pressure (0.05 mmHg) for 48 h to yield 6.2g (at least 1.2 g of

iodine uptake) of dark black powder. For the second step, the IGnPs (5.0 g) and stainless steel balls (500 g, diameter: 5 mm) were charged in the capsule. After five cycles of argon charge/discharge, sulfur trioxide (9.0g, Aldrich Chemical Inc.) was injected through gas inlet. The capsule was agitated with 500 rpm for 24 h and worked-up as following the procedure used for IGnPs to produce ISGnP (4.57g) of dark black powder.

2.4 Electro-chemical study

Cyclic voltammetry (CV) measurements were performed using a computer-controlled potentiostat (CHI 760 C, CH Instrument) in a standard three-electrode cell. Samples/glassy carbon electrodes were used as the working electrode, a platinum wire as the counter electrode, and an Ag/AgCl (saturated KCl) electrode as the reference electrode. Rotating disk electrode (RDE) experiments were carried out on a MSR-X electrode rotator (Pine Instrument) and the CHI760C potentiostat. For all CV and RDE measurements, an aqueous solution of KOH (0.1 M) was used as the electrolyte. N₂ or O₂ was used to purge the solution to achieve oxygen-free or oxygen-saturated electrolyte solution. Procedures for the pretreatment and modification of glassy carbon electrode are described as follows: the working electrode was polished with alumina slurry to obtain a clean surface and washed with deionized water and dried in air. Samples (2 mg) were dissolved in 1 mL solvent (N-methyl-2-pyrrolidone). The sample suspensions were pipetted as much as 10 μ g on the glassy carbon electrode surface, followed by drying at room temperature and Nafion was coated on the electrode surface. The detailed kinetic analysis was conducted according to Koutecky-Levich plots:

$$\frac{1}{j} = \frac{1}{j_k} + \frac{1}{B\omega^{0.5}} \quad (1)$$

Where j_k is the kinetic current and B is Levich slope which is given by:

$$B = 0.2nF(D_{O_2})^{2/3}\nu^{1/6}C_{O_2} \quad (2)$$

n is the number of electron transfer in the reduction of one O₂ molecule. F is the Faraday constant ($F=96485\text{C/mol of e}$), D_{O_2} is the diffusion coefficient of O₂ ($D_{O_2}=1.9 \times 10^{-5} \text{ cm}^2 \text{ s}^{-1}$), ν is the kinematics viscosity of KOH ($\nu = 0.01\text{cm}^2\text{s}^{-1}$) and C_{O_2} is the concentration of O₂ in the solution ($C_{O_2} = 1.2 \times 10^{-6} \text{ mol cm}^{-3}$). The constant 0.2 is adopted when the rotation speed is expressed in rpm.

III. Results and discussion

3.1 Structural information

3.1.1 Functionalization of graphite via ball-mill and Morphology of pristine graphite and IS-graphite

Iodine/sulfonic acid co-doped graphene nanoplatelets (ISGnP) was prepared by sequential ball-milling graphite in the presence of iodine and sulfur trioxide (**Figure 1a**). In the first ball-milling step, edge-selectively iodine doped GnP (IGnP) was prepared by ball-milling graphite (100 mesh, < 150 μ m) in the presence of iodine. In the second ball-milling step, the intermediate IGnP was further grinded in the presence of sulfur trioxide in the ball-mill crusher to yield ISGnP (see Experimental section). As described in **Figure 1a**, the mechanism of edge-selective functionalization *via* mechanochemical ball-milling can be explained that the reactive carbon species (mostly radicals or ions) are generated by cleavage of graphitic C-C bonds at the broken edges.^{5,11} The reactive carbon species reacted with iodine for IGnP and subsequently with sulfur trioxide for ISGnP during sequential ball-milling. After ball-milling, the remnant active carbon species could be terminated by exposure to air moisture and Soxhlet extraction with aqueous medium introducing additional hydroxyl (-OH) and carboxylic acid (-COOH) at the edges of the ISGnP.^{5,11} Scanning electron microscope (SEM) images show that obvious morphology changes before (pristine graphite, **Figure 1b**) and after ball-milling (ISGnP, **Figure 1c**). The pristine graphite displays a large flake shape with grain size in the range of few tens of micrometers (**Figure 1b**). On the other hand, the ISGnP shows aggregated morphology with wrinkled surface due probably to polar nature of sulfonic acid at the edges and reduced grain size in the range of 0.1-1 μ m as a result of mechanochemical cracking (**Figure 1c**).

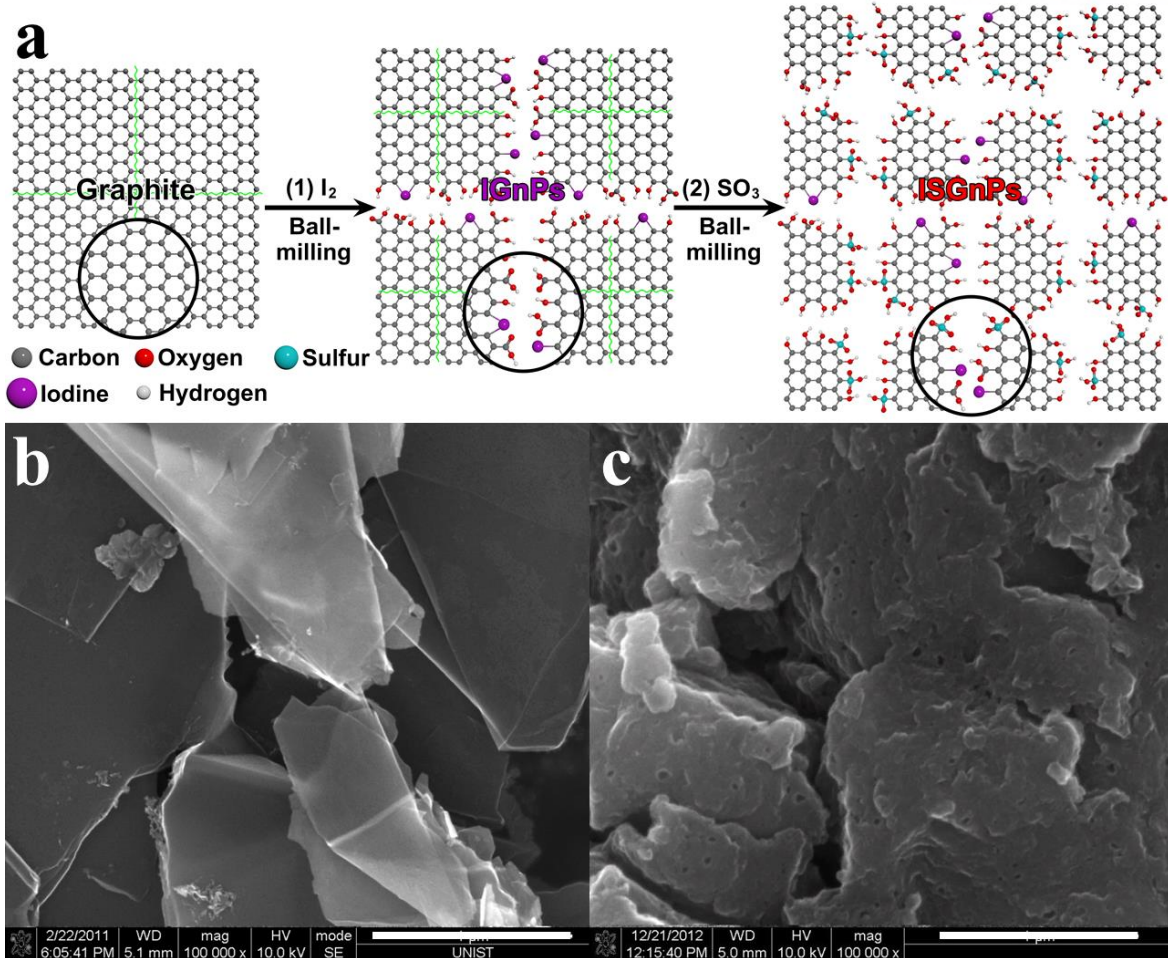


Figure 1. (a) Schematic representation of stepwise ball-milling graphite in the presence of (1) iodine and (2) sulfur trioxide to produce ISGnPs. SEM images: (b) pristine graphite; (c) ISGnP. Scale bars are 1 μ m.

3.1.2 FT-IR study

To illustrate the bonding nature of ISGnP, FT-IR analysis was represented in **Figure 2**. A broad O-H stretching peak is observed at around 3425 cm^{-1} , due to bound moisture and sulfonic acid ($-\text{SO}_3\text{H}$). The peaks at 2920 and 2850 cm^{-1} are due to sp^3 and sp^2 C-H stretching, respectively. The C=O and C-O stretching peaks from carboxyl acid ($\text{O}=\text{C}-\text{OH}$) are located at 1715 and 1230 cm^{-1} , respectively. The C=C stretching peak corresponding to the extended conjugated C=C bond of graphitic framework is at 1585 cm^{-1} . The S=O and S-O stretching peaks for $-\text{SO}_3\text{H}$ were appeared at 1400 and 825 cm^{-1} , respectively. The relatively weak bands of the $-\text{SO}_3\text{H}$ can be interpreted because of the perturbation of the strong inter- and intra-molecular hydrogen bonding.¹⁴ Finally, the C-I stretching peak is detected at around 600 cm^{-1} . The FT-IR results indicate that iodine and sulfonic acid have been introduced in ISGnP via mechanochemical ball-milling.

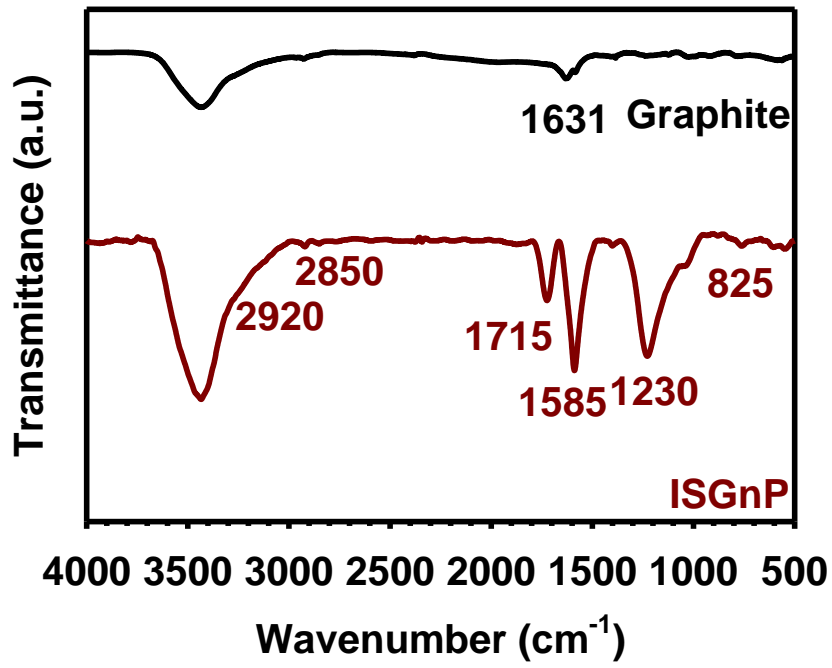


Figure 2. FT-IR spectra.

3.1.3 Elemental analysis (EA), X-ray photoelectron spectroscopy (XPS) and Energy dispersive X-ray (EDX) study

Element compositions of ISGnP were further characterized by using elemental analysis (EA), energy dispersive X-ray (EDX) and X-ray photoelectron spectroscopy (XPS). As summarized in **Table 1**, element compositions are presented in terms of weight percent (wt.%) for EA, atomic percent (at.%) for EDX and XPS. Carbon content of pristine graphite was in the range of 98.35 - 99.64%, while that of ISGnP was significantly reduced in the range of 74.52 - 83.55%, implying that heteroatoms should be introduced at the edges of ISGnP. It could identify the presence of iodine and sulfur, together with oxygen (**Table 1**). X-ray photoelectron spectroscopy (XPS) survey of ISGnP also displays the presence of iodine and sulfur elements (**Figure 3**). The high-resolution XPS spectra show that the C 1s core level of ISGnP is divided into five curves at 284.3 (C=C), 285.1 (C-O), 289.5 (C-S), 288.2 (C=O) and 290.1 (C=C plasmon) (**Figure 4a**). The O 1s core level of ISGnP can be deconvoluted into two curves at 531.4 (O-C=O, S=O), 533 (C-O-H) (**Figure 4b**). The S 2p core level of ISGnP is divided into three peaks at 163.3 (C-S), 164.5 (C-S) and 167.6 (S=O) (**Figure 4c**). The I 3d core level of ISGnP gives four peaks at 618.8 (C-I semi-ionic, $I_{d5/2}$), 620.8 (C-I covalent, $I_{d5/2}$), 630 (C-I semi-ionic, $I_{d3/2}$) and 631.5 (C-I covalent, $I_{d3/2}$) (**Figure 4d**).¹⁶

Table 1. TGA residue amount (%) in N₂ flow at 800 °C, 1000 °C respectively and EA, EDX, XPS of the pristine graphite and ISGnP

Sample	TGA Char Yield in N ₂		Element	EA (wt.%)	EDX (at.%)	XPS (at.%)
	800 °C	1000 °C				
Graphite	99.7	99.1	C	99.64	98.80	98.35
			O	0.13	1.20	1.65
IGnP			C			
			H			
			O			
			I			
ISGnP	73.4	71.7	C	74.52	81.69	83.55
			H	0.84	-	-
			O	17.37	16.20	13.17
			I	-	0.51	0.16
			S	3.76	5.57	1.50

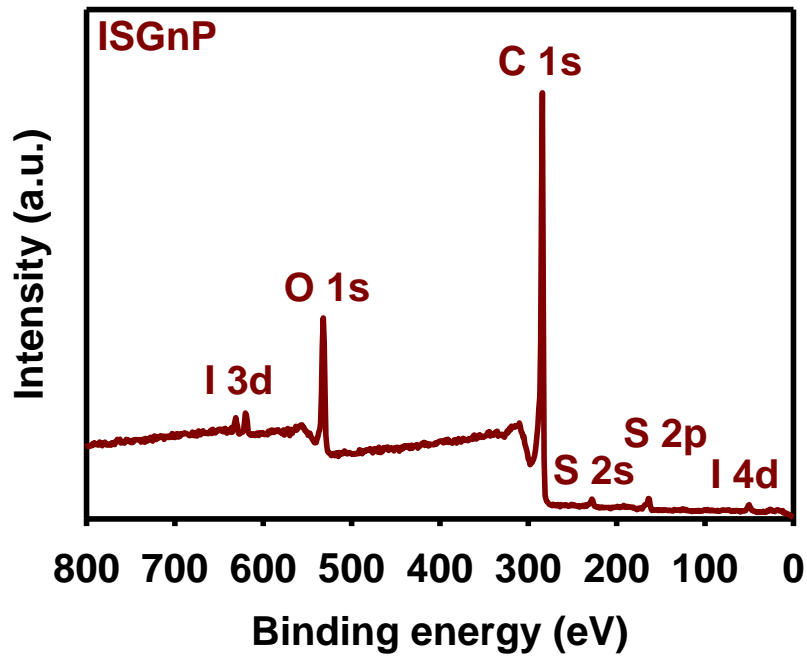


Figure 3. XPS survey spectrum

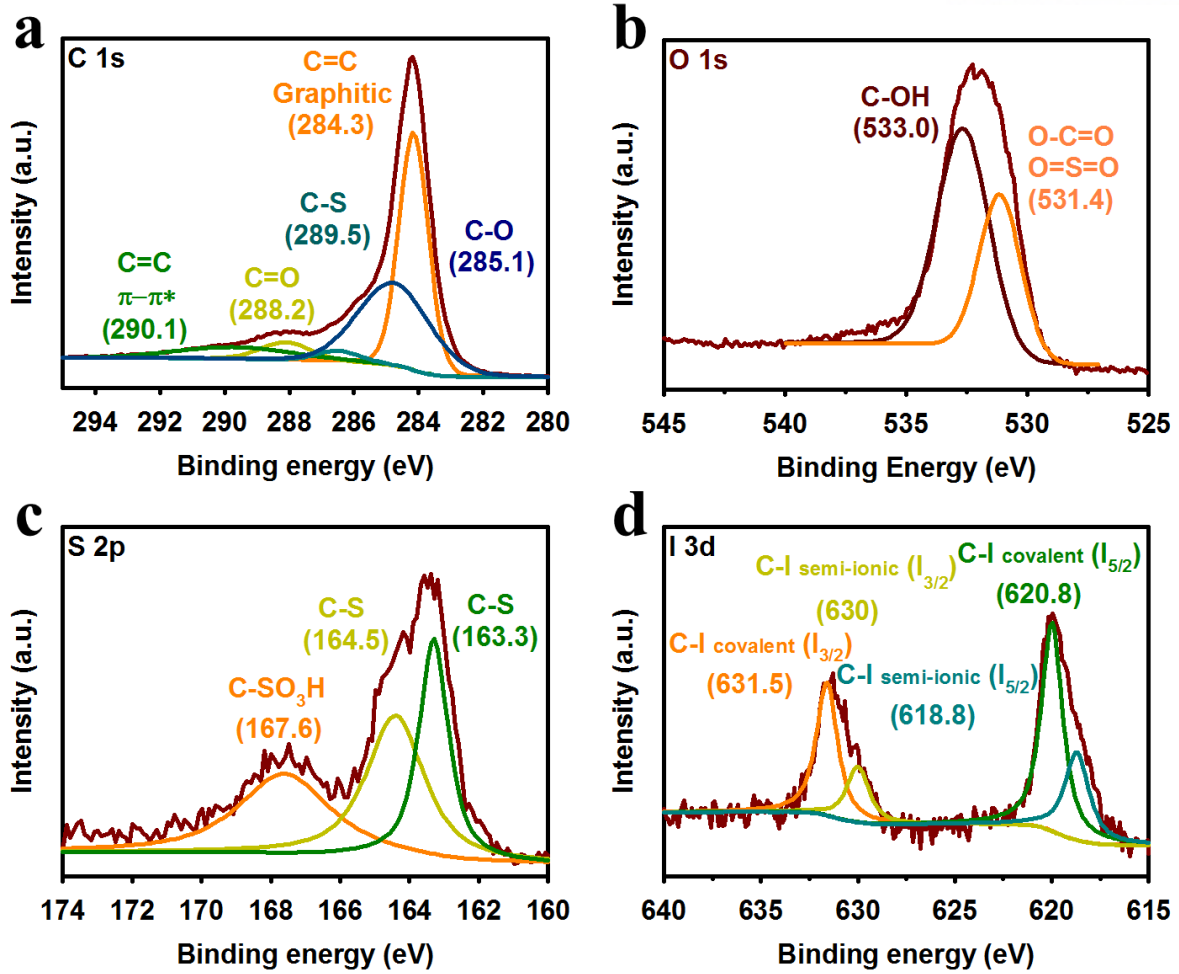


Figure 4. High-resolution XPS survey spectra of the ISGnP: (a) C 1s; (b) O 1s; (c) S 2p; (d) I 3d.

3.1.4 Thermal properties (Thermogravimetric analysis (TGA))

Thermogravimetric analysis (TGA) was conducted to quantitatively estimate the degree of functionalization. Pristine graphite was stable up to 750 °C at one atmosphere. Weight loss of ISGnP occurred around 100 °C, and major thermo-oxidative weight loss occurred at around 480 °C (**Figure 5a**). The early weight loss could be attributed to bound moisture, and the catastrophic weight loss at around 480 °C could be related to heavy functionalization and grain-size reduction of ISGnP. In nitrogen, the pristine graphite experienced negligible weight loss (~0.9 wt.%) up to 1000 °C. On the basis char yield at 1000 °C, the difference between structurally robust, pristine graphite and ISGnP could provide a rough estimation of the amount of functional groups (28.3 wt.% - **Table 1**). The weight loss for ISGnP was mainly attributed to the thermal decomposition of the edge functional groups *via* dehydration, decarboxylation, de-sulfonation and de-iodination into moisture, carbon dioxide, sulfur trioxide and iodine; in that order.^[16] The weight loss (28.3 wt.%) determined by the TGA analysis agreed quite well with the EA result (25.5 wt.%) (**Table 1**).

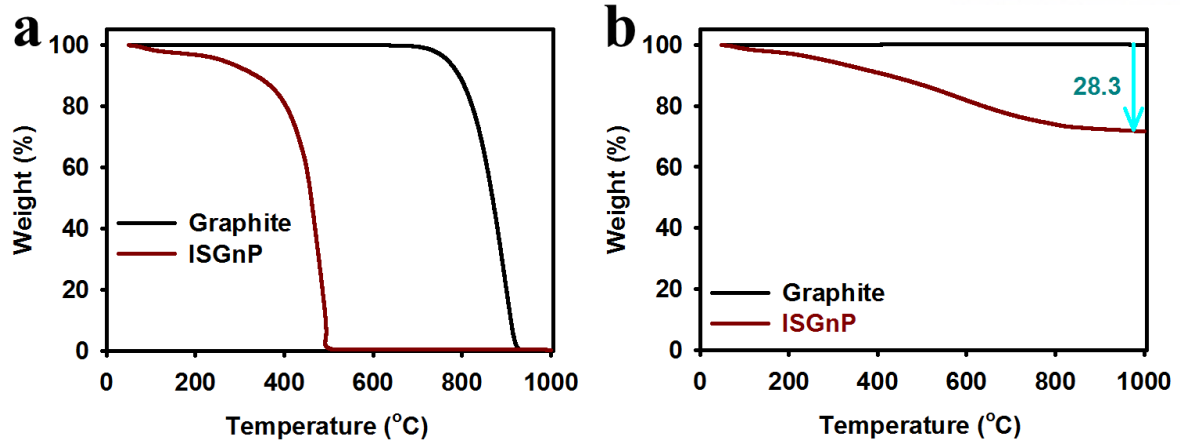


Figure 5. TGA results obtained at the rate of 10 °C/min: (a) in air; (b) in nitrogen.

3.1.5 Raman spectroscopy study

Raman spectra are shown in **Figure 6**. Due to its undisturbed large grain size of the pristine graphite, it does not show the D band (Defect induced band) around 1350 cm^{-1} related to the edge distortion of graphene and other topological defects (**Figure 6**). In contrast, ISGnP shows a strong D band at 1350 cm^{-1} with the I_D/I_G ratio of 1.14, which indicates that mechanochemical cracking by ball-milling has induced significant size reduction, and thus edge distortion of ISGnP as described in **Figure 1**.¹⁴

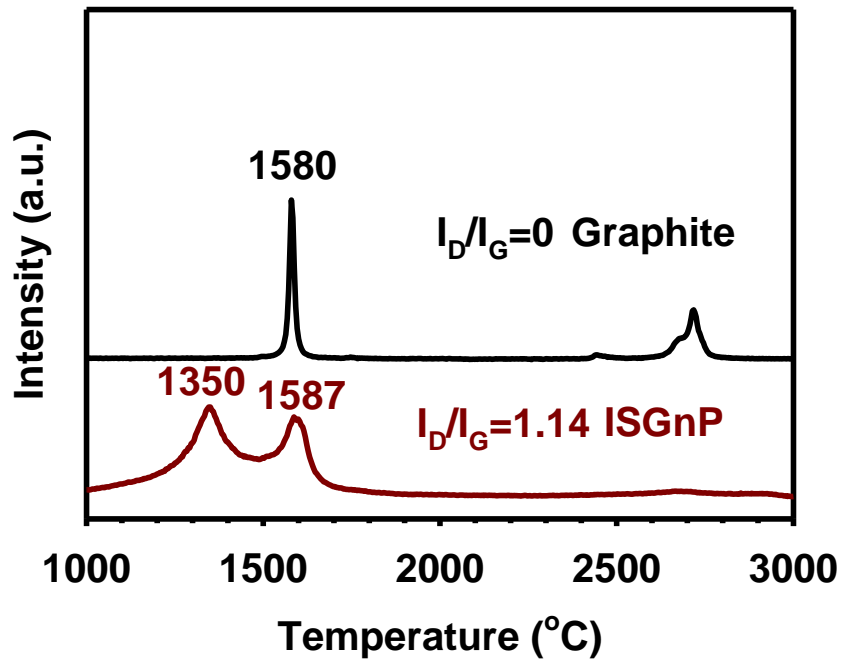


Figure 6. Raman spectrum.

3.1.6 X-ray diffraction (XRD) study

X-ray diffraction (XRD) was used to estimate the degree of delamination of ISGnP (**Figure 7**). The XRD pattern of the pristine graphite showed a typical strong [002] peak at 26.5° associated with an interlayer d -spacing of 0.34 nm of hexagonal graphite.¹⁷ In contrast, ISGnP shows a weak (less than 0.01% of pristine graphite) and broad peak at around 25.7° (d -spacing of 0.35 nm, inset in **Figure 7**), signifying an edge-delamination of graphitic layers after functionalization even in the solid state.¹⁴ Therefore, the ball-milling induces not only mechanochemically cracking large graphitic layers into small fragments but also functionalization at cracked edges, resulting in significant delamination of graphitic layers into GnP.¹⁴ Further exfoliation of ISGnP upon dispersion in solvents could be expected.

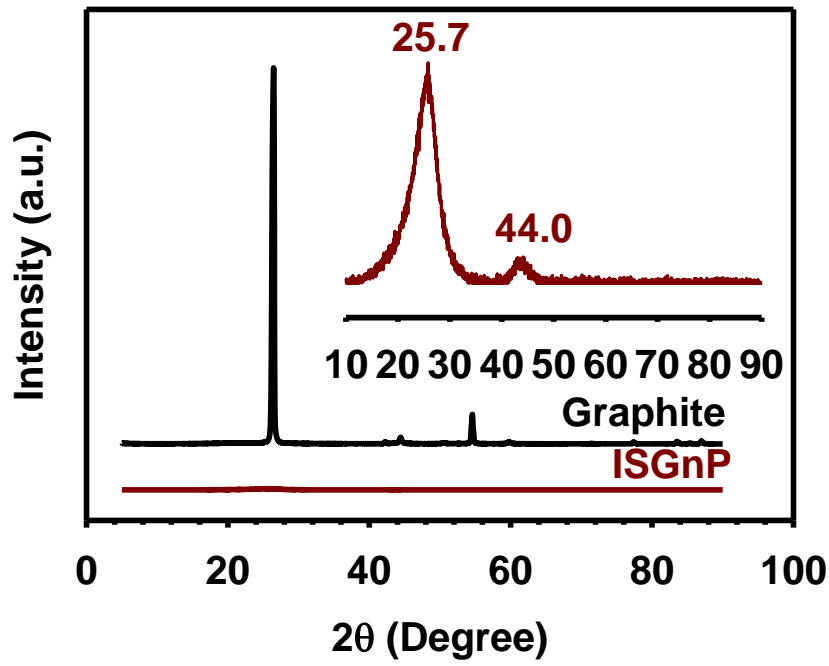


Figure 7. XRD results

3.1.7 Dispersion stability test, Zeta-potential Study, Contact angle study

Figure 8a demonstrates that ISGnP is dispersible well in various solvents not only in aqueous media (small oval) such as water and aqueous ammonium hydroxide, but also polar protic and aprotic solvents (large oval) such as alcohols, acetone, N,N-dimethylformamide (DMF), N,N-dimethylacetamide (DMAc), N-methyl-2-pyrrolidone (NMP). Due to the presence of polar acidic edge-functional groups at the edges of ISGnP including OH, COOH and SO₃H, ISGnP displays a poor dispersibility in aqueous acidic medium and nonpolar solvents such as aqueous hydrochloric acid, toluene, dichloromethane and hexane, and ether solvents. The dispersion stability of ISGnP in NMP was evaluated by Zeta potential measurement. The values are -43.4, -45.4 and -43.6 mV at different concentrations of 0.4, 0.5 and 0.6 mg/mL, respectively (**Table 2**). The result indicated that the negatively charged sulfonate groups (-SO₃⁻) from sulfonic acids were contributed to a good dispersion stability of ISGnP in basic NMP medium. Hence, the high dispersion stability of ISGnP allows a good solution processability, leading to many practical applications. **Figure 8b** shows contact angle snapshot, which is describing for polar surface natures of ISGnP. Generally, if the water contact angle is larger than 90°, the solid surface is considered hydrophobic.¹⁸ ISGnP has contact angle of 51°, it is considered to be hydrophilic as like the surface of silicon oxide (SiO₂) (**Figure 8c**). Although the ISGnP was expected to possess more hydrophilic nature than SiO₂ due to the polar functional groups at its edges such as (OH, COOH, SO₃H), it displayed higher contact angle than SiO₂. This is because of the presence of much less hydrophilic iodine, which repels water molecules to minimize its contact area with the surface of ISGnP. As a result, the interaction between the ISGnP and water was diminished and its contact angle was less than silicon wafer.

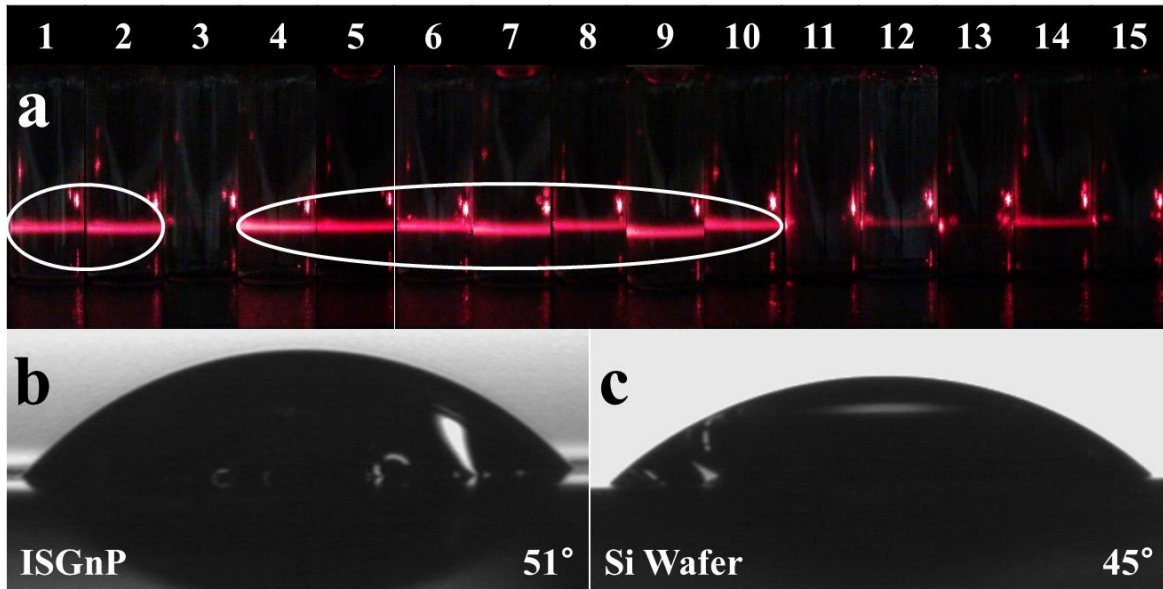


Figure 8. Photographs of ISGnP dispersed solutions in various solvents after one week standing on bench top in the normal laboratory condition: (a) (1) H₂O; (2) 1M aq. NH₄OH; (3) 1M aq. HCl; (4) MeOH; (5) EtOH; (6) ethyl acetate; (7) acetone; (8) DMAc; (9) DMF; (10) NMP; (11) toluene; (12) CH₂Cl₂; (13) hexane; (14) diethyl ether; (15) THF. Contact angles: (b) the surface of ISGnP coated on Si wafer; (c) the surface of Si wafer. The contact angle is an average value of ten measurements.

Table 2. Zeta-potential of samples at different concentrations in NMP solution

Sample	Concentration (mg/mL)		
	0.4	0.5	0.6
IGnP	-38.7	-38.5	-34.8
ISGnP	-43.4	-45.4	-43.6

Table 3. The relationship between Zeta-potential and colloidal stability*

Zeta-potential (mV)	Stability behavior of the solid
From 0 to ± 5	Rapid coagulation or flocculation
From ± 10 to ± 30	Incipient instability
From ± 30 to ± 40	Moderate stability
From ± 40 to ± 60	Good stability
More than ± 61	Excellent stability

* http://en.wikipedia.org/wiki/Zeta_potential.

3.2 Application (Oxygen reduction reaction)

3.2.1 Cyclic voltammetry (CV)

Given the structural information, ISGnP was finally evaluated for potential use as an electro-catalyst in fuel cells. The heteroatoms in ISGnP (e.g., iodine, sulfur and oxygen) could polarize ISGnP to enhance electro-catalytic activity.^[22] Polar heteroatom-doping enables stable adsorption onto the surface of functionalized graphitic electrodes (thermodynamic contribution)^[19] and rapid oxygen diffusion to the electrode (kinetic contribution).^[16] For the purpose of comparison, the pristine graphite (much bigger grain size than ISGnP), edge-hydrogen functionalized GnP (HGnP,^[16] similar grain size with ISGnP) and platinum on activated carbon (Pt/C, Vulcan XC-72R, commercial ORR electro-catalyst) were tested under the same conditions. The HGnP was prepared *via* ball-milling of graphite under H₂ gas.^[16] Typical, cyclic voltammograms (CV) in alkaline electrolyte showed that ISGnP has much better electro-chemical capacitance than pristine graphite and nitrogen-saturated HGnP (**Figure 9a** and **Table 4**). The capacitance of ISGnP (108.8 F/g) is even better than Pt/C (90.1 F/g). When oxygen saturated, ISGnP displays superb electro-catalytic activity; in relation to the reference samples (**Figure 9b** and **Table 4**). In addition, ISGnP showed significantly improved onset potential (of ORR) compared to pristine graphite and HGnP (sky blue arrow, **Figure 9b**). This expected result implies that ISGnP contributes to efficient oxygen diffusion and adsorption. For example, the BET surface area of ISGnP (6.03 m²/g) is much less than that of HGnP (437 m²/g), but the specific capacitance of ISGnP is much greater (**Table 5**). This can be explained by the high polarity of the ionic iodine (C-I⁺-C) and sulfonate (-SO₃⁻) of ISGnP in the alkaline medium; which contribute to increased double-layer capacitance by enhancing charge polarization (thermodynamics)^[10] and oxygen diffusion (kinetics).^[16] Together, these overcome the disadvantage of its small surface area. More importantly, the ISGnP showed better cycle stability than Pt/C under prolonged use (10,000 cycles). ISGnP exhibited capacitance retentions of 77.1 and 66.4% under nitrogen and oxygen-saturated conditions respectively, while Pt/C retained only 57.7 and 53.4% (**Table 6**).

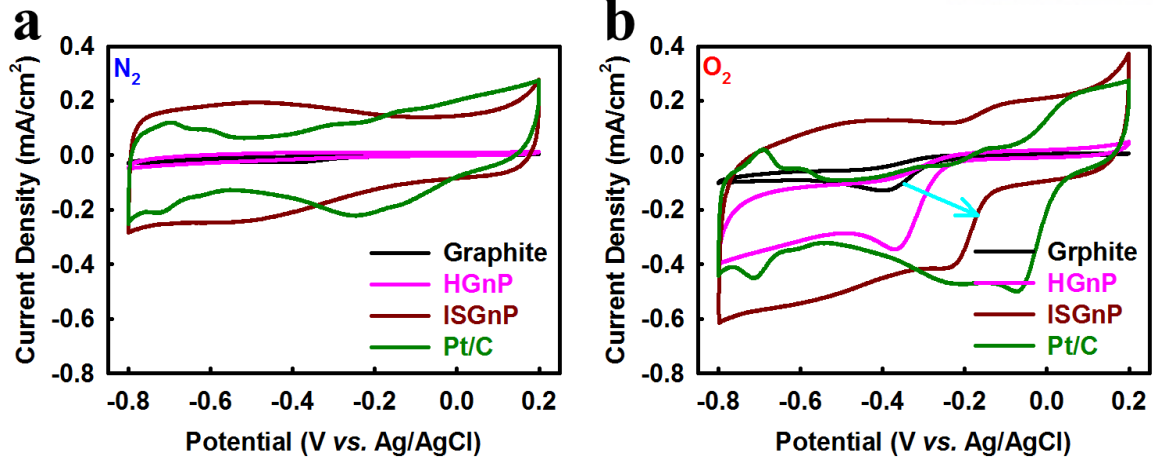


Figure 9. Cyclic voltammograms (CV) of samples on glassy carbon (GC) electrodes in 0.1 M aq. KOH solution; with scan rate of 10 mV/s: (a) Nitrogen-saturated; (b) Oxygen-saturated.

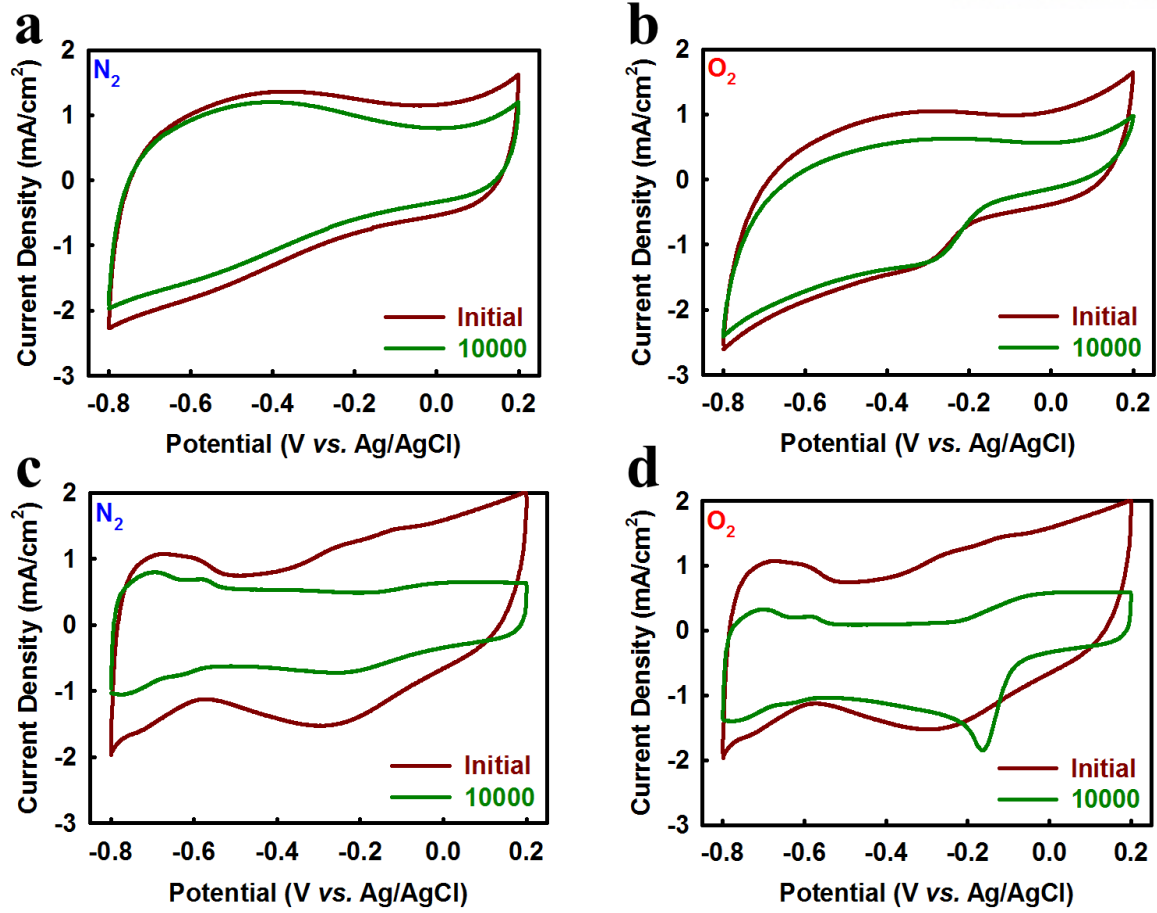


Figure 10. Comparison of cyclic voltammograms (CV) of samples on glassy carbon (GC) electrodes in 0.1 M aq. KOH solution with scan rate of 100 mV/s: (a) ISGnP in nitrogen-saturated condition; (b) ISGnP in oxygen-saturated condition; (c) Pt/C in nitrogen-saturated condition; (d) Pt/C in oxygen-saturated condition.

Table 4. The specific capacitance (F/g) obtained from average value of 100 cycles

Sample	Capacitance (F/g)	
	N ₂	O ₂
Pristine graphite	3.5	11.0
HGnP	6.69	34.7
ISGnP	108.8	153.5
Pt/C	90.1	104.2

Table 5. BET surface areas of samples

Sample	Surface area (m ² /g)	Pore volume (mL/g)	Pore size (nm)
Pristine graphite	2.78	0.0016	22.7
HGnP*	437	0.3909	35.8
ISGnP	6.03	0.0205	13.58

* Adapted from Jeon, et al., *J. Am. Chem. Soc.* 2013, 135, 1386-1393.

Table 6. The cycle retention after 10000 cycles in oxygen- and nitrogen-saturated 0.1M aq. KOH electrolyte at the scan rate of 100 mV/s

Sample	Retention after 10000 cycles (%)	
	N ₂	O ₂
Graphite	99.0	91.8
ISGnP	77.1	66.4
Pt/C	57.7	53.4

3.2.2 Rotating disk electrode (RDE)

The ORR kinetics of ISGnP were studied using a rotating disk electrode (RDE) and analyzed using the Koutecky–Levich equation (Supporting Information). **Figure 11** shows that the current density increases as the rotation rate increases, because the flux of electro-active species to the surface of the electrode increases by convection force. As summarized in **Table 7**, the electron transfer number (n) of the ISGnP was increased from 2.8 to 4.0 as the applied potential increased from -0.4 to -0.6 V; which is a typical potential range of fuel-cell operation.^[23] This result indicates that use of ISGnP as an electro-catalyst could efficiently facilitate ORR. Hence, introduction of iodine (I) and sulfonic acid (-SO₃H) at the edges of graphitic layers was found to produce good ORR performance; with higher capacitance and better cycle stability than commercial Pt/C electro-catalyst. These results provide insights into the design of carbon-based materials as alternatives to expensive Pt-based electro-catalysts for cathodic ORR in fuel cells.

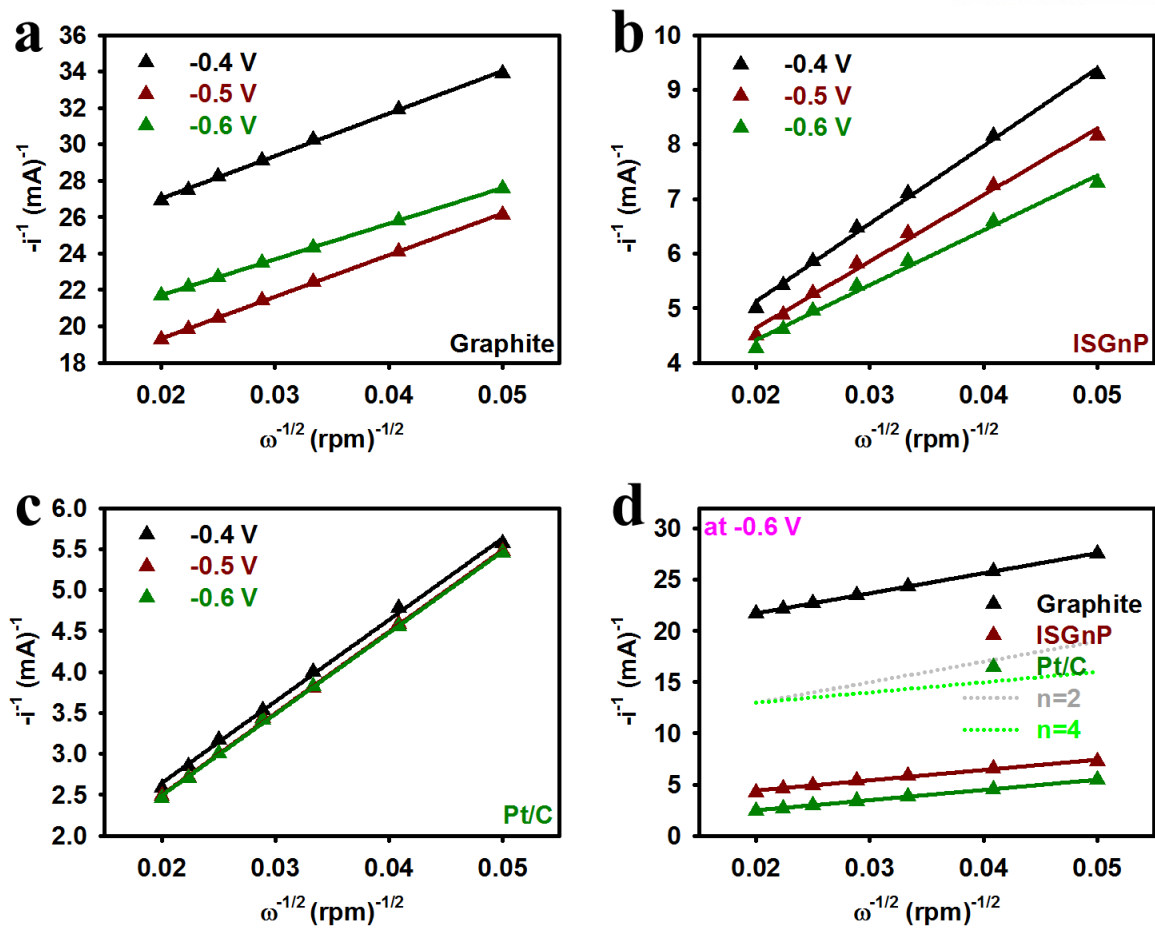


Figure 11. Koutecky-Levich plots derived from RDE measurements at different electrode potentials: (a) Pristine graphite; (b) ISGnP; (c) Pt/C; (d) Comparison of the Koutecky-Levich plots at -0.6 V electrode potential. ISGnP and Pt/C are a four-electron transfer process, while the pristine graphite is close to a classical two-electron process.

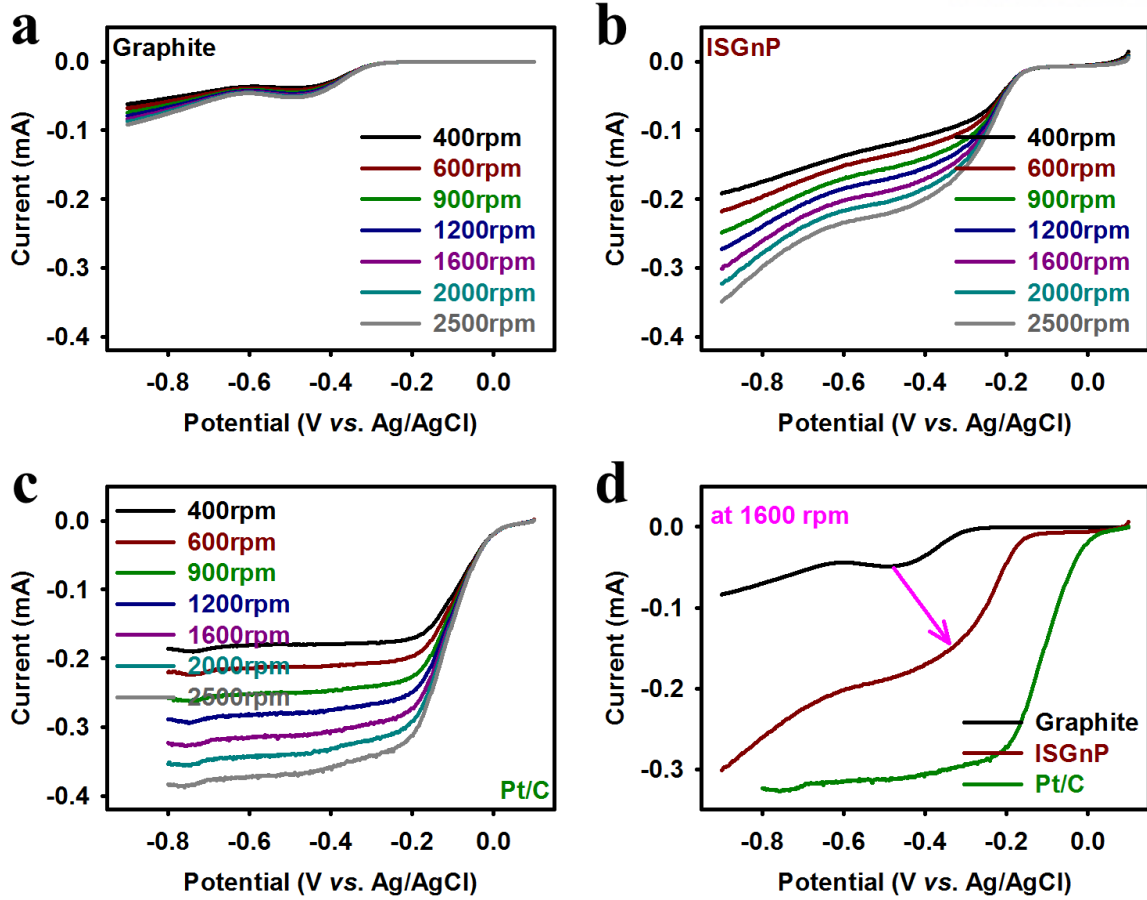


Figure 12. RDE voltammograms in oxygen-saturated 0.1 M aq. KOH solution with a scan rate of 10 mV/s at different rotating rates of 400, 600, 900, 1200, 1600, 2000 and 2500 rpm: (a) the pristine graphite; (b) ISGnP; (c) Pt/C; (d) comparison of RDE voltammograms of sample electrodes at a rotation rate of 1600 rpm.

Table 7. The average number of electrons (n) transferred for oxygen reduction reaction at different potential for sample electrodes in oxygen-saturated 0.1M aq. KOH electrolyte

Sample	Potential (V)		
	-0.4	-0.5	-0.6
Graphite	1.7	1.7	2.0
ISGnP	2.8	3.3	4.0
Pt/C	3.9	4.0	4.0

IV. Conclusion

The interesting properties of graphene, together with its low price, potential application for new commercialization, have emerged the next-generation research area for alternative energy system studies and technological applications. Specifically, the introduction of hetero-atom into graphene nanoplatelets can be excellent, efficient breakthrough to broaden and strengthen the electronic function, performance in electro-chemical devices such as fuel cells. The hetero-atom doped graphene-based nano-material has been studied to introduce the newly advanced electro-catalyst in fuel cells. It should be vital things to achieve theoretical research of highly active materials for ORR performance to jump up existing limitations. It has been shown as an organic catalyst based on the molecular control engineering, also as a platinum catalyst support material. Scientist engineer have shown the special properties of graphene (theoretical huge surface area, good electrical, thermal conductivity, stability). Futhermore, graphene can conduct the synergistic performace between graphene and other atoms, molecules. These points were attributed to the excellent electro-chemical performance in fuel cells.

As one of these instances, it was able to synthesize edge-iodine/sulfonic acid-functionalized, graphene nano-platelets (ISGnP) *via* stepwise ball-milling of graphite with iodine initially and subsequently with sulfur trioxide. The structure of the resultant ISGnP was confirmed by various microscopic and spectroscopic analyses. Due to the polar functional groups, the dispersibility of ISGnP in various polar solvents is good enough for solution processing to form electrodes. Due to hetero-atom doping to enhance the polarity and oxygen-diffusion, the ISGnP displayed superior electro-catalytic activity for ORR; compared to commercial Pt/C. The thermodynamic control of ORR contributed to enhanced oxygen adsorption and electron transfer. These were induced by edge-functional groups (iodine and sulfonic acid) on the graphitic framework, and the kinetic contribution (related to oxygen diffusion by the polar nature) of these edge functional groups. More importantly, ISGnP displayed better cycle stability; compared with Pt/C. Considering scalable productivity, edge-selectivity and manufacturing simplicity, the ball-milling approach is considered to be an eco-friendly, low-cost, simple general method; when compared to existing GO/rGO and CVD approaches. Hence, ISGnP appears to be a strong potential alternative to expensive Pt/C electro-catalyst.

References

-
- ¹ Qu, L.; Liu, Y.; Baek, J. B.; Dai, L. Nitrogen-Doped Graphene as Efficient Metal-Free Electrocatalyst for Oxygen Reduction in Fuel Cells. *ACS Nano*. 2010, 4, 1321–1326.
 - ² Stankovich S, et al. Synthesis of graphene-based nanosheets via chemical reduction of exfoliated graphite oxide. *Carbon*. 2007, 45,1558–1565.
 - ³ Sheng, Z.-H.; Gao, H.-L.; Bao, W.-J.; Wang, F.-B.; Xia, X.-H. Synthesis of Boron-Doped Graphene for Oxygen Reduction Reaction in Fuel Cells. *Journal of Materials Chemistry* 2012, 22, 390-395.
 - ⁴ Long, D.; Li, W.; Ling, L.; Miyawaki, J.; Mochida, I.; Yoon, S.-H. Preparation of Nitrogen-Doped Graphene Sheets by a Combined Chemical and Hydrothermal Reduction of Graphene Oxide. *Langmuir* 2010, 26, 16096-16102.
 - ⁵ Yang, Z.; Yao, Z.; Li, G.; Fang, G.; Nie, H.; Liu, Z.; Zhou, X.; Chen, X.; Huang, S. Sulfur-Doped Graphene as an Efficient Metal-Free Cathode Catalyst for Oxygen Reduction. *ACS Nano* 2012, 6, 205-211.
 - ⁶ Poh, W. L.; Šimek, P.; Sofer, Z.; Pumera, M. Halogenation of Graphene with Chlorine, Bromine, or Iodine by Exfoliation in a Halogen Atmosphere. *Chemistry-A European Journal* 2013, 19, 2655-2662.
 - ⁷ Hummers WS, Offeman RE. Preparation of graphitic oxide. *J Am Chem Soc*. 1958, 80, 1339-1339.
 - ⁸ Fan X, et al. Deoxygenation of exfoliated graphite oxide under alkaline conditions. *Adv Mater*. 2008, 20, 4490-4493.
 - ⁹ Barcerril HA, et al. Evaluation of solution-processed reduced graphene oxide films as transparent conductors. *ACS Nano*. 2008, 2, 463-470.
 - ¹⁰ Park S, Ruoff RS. Chemical methods for the production of graphenes. *Nat Nanotechnol*. 2009, 4, 217-224.
 - ¹¹ In-Yup Jeon, et al. Edge-carboxylated grapheme nanosheets via ball milling. *Proceedings of the National Academy of Sciences*. 2012, 109, 5588-5593.
 - ¹² In-Yup Jeon, et al. Large-Scale Production of Edge-Selectively Functionalized Graphene Nanoplatelets via Ball Milling and Their Use as Metal-Free Electrocatalysts for Oxygen Reduction

Reaction. *J Am Chem Soc.* 2012, 135, 1386-1393.

¹³ Jeon, I.-Y.; Zhang, S.; Zhang L.; Choi, H.-J.; Seo, J.-M.; Xia, Z.; Dai, L.; Baek, J.-B. "Edge-Selectively Sulfurized Graphene Nanoplatelets as Efficient Metal-Free Electrocatalysts for Oxygen Reduction Reaction: The Electron Spin Effect" *Advanced Materials* 2013, 25, 6138-6145.

¹⁴ Seo, J.-M.; Jeon, I.-Y.; Baek, J.-B. "Mechanochemically Driven Solid-State Diels-Alder Reaction of Graphite into Graphene Nanoplatelets" *Chemical Science* 2013, 4, 4273-4277.

¹⁵ Jeon, I.-Y.; Choi, H.-J.; Choi, M.; Seo, J.-M.; Jung, S.-M.; Kim, M.-J.; Zhang, S.; Zhang, L.; Xia, Z.; Dai, L.; Park, N.; Baek, J.-B. "Facile, scalable synthesis of edge-halogenated graphene nanoplatelets as efficient metal-free electrocatalysts for oxygen reduction reaction" *Scientific Reports* 2013, 3, 1810.

¹⁶ Wang Hai-Fang, et al. XPS Study of C-I Covalent Bond on Single-walled Carbon Nanotubes (SWNTs). *Acta Phys. Chim. Sin.* 2004, 20, 673-675.

¹⁷ Li ZQ, et al. X-ray diffraction patterns of graphite and turbostratic carbon. *Carbon* 2007, 45, 1686-1695.

¹⁸ de Gennes, P. G. Wetting: Statics and Dynamics. *Review of Modern Physics* 1985, 57, 827-863.

¹⁹ Chengzhou Zhu. Shaojun Dong. Recent progress in graphene-based nano-materials advanced electro catalysts towards oxygen reduction reaction. *Nanoscale* 5, 1753, doi:10.1039/c2nr33839d (2013).

Bibliography

¹ Alan Filer., Jong-Beom Baek. Two and three dimensional network polymers for electrocatalysis. *Phys. Chem. Chem Phys* 16, 11150, doi: 10.1039/c4cp01246a (2014).

² S. Stankovich., R. S. Ruoff. et al. Graphene-based composite materials. *Nature*. 442, 282-286, doi: 10.1038/nature04969 (2006).

³ Qu. L., Liu. Y., Jong-Beom Baek., Dai L. Nitrogen-doped graphene as efficient metal-free electrocatalyst for oxygen reduction in fuel cells. *ACS Nano*. 4, 1321-1326, doi: 10.1021/nn901850u (2010).

⁴ I. -Y. Jeon., Jong-Beom Baek et al. Edge-carboxylated graphene nanosheets via ball milling. *Proc. Natl. Acad. Sci. U.S.A.* 109, 5588-5593, doi: 10.1073/pnas.1116897109 (2012).

⁵ I. -Y. Jeon., Jong-Beom Baek. et al. Large-scale production of edge-selectively functionalized graphene nanoplatelets via ball milling and their uses as metal-free electrocatalysts for oxygen reduction reaction. *J. Am. Chem. Soc.* 135, 1386-1393, doi: 10.1021/ja3091643 (2013).

⁶ Xiang-Kai Kong., Chang-Le Chen., Qian-Wang Chen. Doped graphene for metal-free catalysis. *Chem. Soc. Rev.* 43, 2841, doi: 10.1039/c3cs60401b (2014).

⁷ Nick Daems., Xia Sheng., Ivo F. J. Vankelecom and Paolo P. Pescarmona. Metal-free doped carbon materials as electrocatalysts for the oxygen reduction reaction. *Journal of Materials Chemistry A*. 2, 4085, doi: 10.1039/c3ta14043a (2014).

⁸ Da-Wei Wang., Dangsheng Su. Heterogeneous nanocarbon materials for oxygen reduction reaction. *Energy Environ. Sci.* 7, 576, doi: 10.1039/c3ee43463j (2014).

Acknowledgement

석사생활, 2년의 시간이 훌쩍 지나서 어느덧 졸업을 하게 되었습니다. UNIST에서의 길고 긴 생활의 마침표를 찍게 되어 뿌듯하기도 하고 아쉽기도 합니다.

UNIST에 들어오고 졸업하기까지 저를 정신적으로 지지해주셨던 부모님에게 감사합니다. UNIST 입학 시 반신반의 했던 저에게 도전해보라고 조언을 해주셨고 제가 어떤 일을 하더라도 끝까지 믿어주셨습니다. 그러한 믿음이 저에게 매 순간마다 동기부여가 되었고 좋은 결과들이 생겼던 것 같습니다.

지도교수님이신 백종범교수님께 감사 드립니다. 2년의 대학원 생활 동안에 여러 인생 경험, 대학원 생활할 때 주의할 점, 전공분야 전문지식을 저에게 가르쳐주셨습니다. 때론 쓰긴 했지만 약이 되었던 것 같습니다. 교수님의 말씀을 새겨듣고 학교 밖에 나가서도 잘해내겠습니다.

연구실 인엽이형, 현정누나, 서윤누나, 선민누나, 정민누나, 민정누나, 석진이, 자비드에게도 감사드립니다. 생소한 대학원 생활에서 연구지식, 인생조언과 같은 많은 것을 저에게 해주셨습니다.

인엽이형께서는 포닥 후 앞으로 원하시는 직업과 재미있는 일을 하셨으면 합니다. 그리고 셋째를 위해서 운동을 틈틈이 하시며 건강관리도 하셨으면 합니다.

누나들도 박사과정 연구 재미있게 하시고 원하시는 결과를 얻으시길 바라요. 힘든 일이 있어도 긍정적으로 마음 가지며 지내길 바랄게요. 그리고 2015년에는 일뿐 만 아니라 사랑도 모두 쟁취하시길 바랄게요.

석진이도 대학원 생활 동안 앞으로 많은 것을 배우고 열심히 공부해서 보람 있는 대학원 생활 하길 바란다. 너에게 좋은 점만 가지고 나쁜 것을 빨리 쉽게 떨쳐버리며 대학원 생활을 하면 좋은 결과가 있을 거야.

To Javeed, I really appreciate all the help you've given me. I think I have done experimental things well thanks to you. I wish that you get good career and nice lifetime with your wife.

모두들 감사했습니다. 올 한해 좋은 일이 가득하셨으면 합니다.